Assignment of the Heme Axial Ligand(s) for the Ferric Myoglobin (H93G) and Heme Oxygenase (H25A) Cavity Mutants as Oxygen Donors Using Magnetic Circular Dichroism†

Alycen E. Pond,‡ Mark P. Roach,‡,§ Masanori Sono,‡ Ann Huff Rux,‡ Stefan Franzen,|| Robert Hu,⊥ Melissa R. Thomas,⊥ Angela Wilks,# Yi Dou,@ Masao Ikeda-Saito,@ Paul R. Ortiz de Montellano,# William H. Woodruff,|| Steven G. Boxer,⊥ and John H. Dawson*,‡,▽

Department of Chemistry and Biochemistry, University of South Carolina, Columbia, South Carolina 29208, Department of Structural Molecular Science, Institute of Molecular Science, Okazaki, Myodaiji, 444 Japan, Los Alamos National Laboratory, CST-4 MS G758, Los Alamos, New Mexico 87545-0001, Department of Chemistry, Stanford University, Stanford, California 94305-5080, Department of Pharmaceutical Chemistry, School of Pharmacy, University of California, San Francisco, California 94143-0446, Department of Physiology and Biophysics, Case Western Reserve University, Room E559, School of Medicine, Cleveland, Ohio 44106-4970, and School of Medicine, University of South Carolina, Columbia, South Carolina 29208

Received October 23, 1998; Revised Manuscript Received March 8, 1999

ABSTRACT: UV−visible absorption and magnetic circular dichroism (MCD) data are reported for the cavity mutants of sperm whale H93G myoglobin and human H25A heme oxygenase in their ferric states at 4 °C. Detailed spectral analyses of H93G myoglobin reveal that its heme coordination structure has a single water ligand at pH 5.0, a single hydroxide ligand at pH 10.0, and a mixture of species at pH 7.0 including five-coordinate hydroxide-bound, and six-coordinate structures. The five-coordinate aquo structure at pH 5 is supported by spectral similarity to acidic horseradish peroxidase (pH 3.1), whose MCD data are reported herein for the first time, and acidic myoglobin (pH 3.4), whose structures have been previously assigned by resonance Raman spectroscopy. The five-coordinate hydroxide structure at pH 10.0 is supported by MCD and resonance Raman data obtained here and by comparison with those of other known five-coordinate oxygen donor complexes. In particular, the MCD spectrum of alkaline ferric H93G myoglobin is strikingly similar to that of ferric tyrosinate-ligated human H93Y myoglobin, whose MCD data are reported herein for the first time, and that of the methoxide adduct of ferric protoporphyrin IX dimethyl ester (Fe^{III}PPIXDME). Analysis of the spectral data for ferric H25A heme oxygenase at neutral pH in the context of the spectra of other five-coordinate ferric heme complexes with proximal oxygen donor ligands, in particular the *p*-nitrophenolate and acetate adducts of Fe^{III}PPIXDME, is most consistent with ligation by a carboxylate group of a nearby glutamyl (or aspartic) acid residue.

Heme proteins with protein-derived oxygen donor proximal ligands are relatively rare in nature. The best known example of such ligation is that of bovine liver catalase which contains a tyrosine phenolate proximal heme iron ligand (*1*). In addition, a series of naturally occurring hemoglobin mutants having distal or proximal histidines replaced by tyrosine or glutamate (the M hemoglobins) have been established by X-ray crystallography (*2*−*4*) and resonance Raman spectroscopy (*5*, *6*) to have phenolate or carboxylate ligation. Other proteins with tyrosinate and glutamate oxygen donor ligation have been recently produced by site-directed mutagenesis of various myoglobins (*7*−*10*) and cytochrome *c* peroxidase (*11*).

The use of site-directed mutagenesis techniques has become invaluable in identifying catalytically and structurally important protein residues within a protein system. A relatively new type of mutation, based on altering the size of the amino acid at the point of mutation, substitutes a glycine or alanine for the larger original residue and leaves a cavity within the protein. Termed cavity mutants, these mutated proteins demonstrate the ability to employ exogenous ligands to reconstitute their wild-type activity. This rescue of activity has been seen for the cavity mutants of azurin (*12*), carbonic anhydrase (*13*), hexose-1-phosphate uridyltransferase (*14*), and various heme proteins (*15*−*18*).

† This work was supported by NIH Grants GM 26730 (to J.H.D.), GM 51588 (to M.I.-S.), GM 27738 (to S.G.B.), and DK 30297 (to P.R.O.), and by Los Alamos Bioremediation Grant XAM-1 (to W.H.W.). The electromagnet for the circular dichroism spectrophotometer was purchased through a grant from Research Corp.

* To whom correspondence should be addressed at the Department of Chemistry and Biochemistry, University of South Carolina, 730 S. Main St., Columbia, SC, 29208. Phone: 803-777-7234. Fax: 803-777-9521. Email: Dawson@psc.sc.edu.

‡ Department of Chemistry and Biochemistry, University of South Carolina.

§ Present address: Department of Structural Molecular Science, Institute for Molecular Science, Okazaki, Myodaiji, 444 Japan.

|| Los Alamos National Laboratory.

⊥ Department of Chemistry, Stanford University.

Department of Pharmaceutical Chemistry, University of California at San Francisco.

@ Department of Physiology and Biophysics, Case Western University.

▽ School of Medicine, University of South Carolina.

10.1021/bi9825448 CCC: $18.00
Published on Web 05/11/1999

Several different research groups have recently produced site-directed mutant heme proteins in which the proximal heme ligand, histidine, is replaced with smaller, noncoordinating residues. This approach was pioneered by Barrick (*15*) for sperm whale myoglobin (Mb)[1] and has since been accomplished for cytochrome *c* peroxidase (*16*), heme oxygenase (*17*), and horseradish peroxidase (*18*). Studies of cavity mutants to date have focused on the dynamics of binding unnatural ligands (*19*−*22*) and the resulting effects on catalytic activity (*18*). The structures of the ferric heme cavity mutants have been studied in the cases of H175G cytochrome *c* peroxidase (*16*, *23*) and H25A heme oxygenase (*17*), but have not yet been addressed in detail for H170A horseradish peroxidase or sperm whale H93G Mb. Understanding the nature of these derivatives is an essential part of the complete characterization of the cavity mutant systems and is expected to be the subject of future studies as more cavity mutant proteins are engineered.

The magnetic circular dichroism (MCD) spectra of iron porphyrins are very sensitive to the nature of the axial ligands to the heme iron. Thus, the technique is especially well suited for investigations of axial ligation in structurally undefined heme iron proteins (*24*). Ligation assignments are made through comparisons of the spectra of the structurally uncharacterized heme protein with those of structurally defined heme iron centers. In this manner, MCD spectroscopy has been used to characterize the coordination structure of numerous heme proteins including cytochrome P450cam (*25*), *C. fumago* chloroperoxidase (*25*), *A. ornata* dehaloperoxidase (*26*), *N. lobatus* chloroperoxidase (*26*), and heme oxygenase (*27*). Though catalase (*28*) and synthetic model systems with oxygen donor ligands have been investigated by MCD (*29*−*31*), the technique has yet to be applied to spectrally characterize mutant heme proteins suspected of oxygen donor ligation.

We present herein spectroscopic investigations of exogenous ligand-free ferric sperm whale H93G Mb and human H25A heme oxygenase in the context of known ferric five-coordinate oxygen donor complexes in order to establish their coordination structure and, in so doing, to refine the application of MCD spectroscopy to distinguish various types of oxygen donor ligation encountered in natural and engineered proteins and synthetic model systems. As an essential part of this effort, we also present for the first time MCD data for ferric human H93Y myoglobin and acidic ferric HRP.

EXPERIMENTAL PROCEDURES

Materials. Sperm whale H93G Mb was expressed and purified in the presence of 10 mM imidazole as previously described (*15*). As isolated, the protein contains imidazole as its proximal ligand and exists in a mixture of ferric and oxyferrous states. Complete oxidation of the heme iron is accomplished by addition of a few crystals of potassium ferricyanide (Fluka). Imidazole can be removed from the proximal pocket by two different methods. Gel filtration through a P6DG (BioRad) size exclusion column typically removes approximately 90% of iron-bound imidazole as judged by resonance Raman spectroscopy (*32*). Extraction of the heme from H93G Mb, followed by reconstitution with hemin, yields ferric H93G Mb completely free of imidazole (*32*). Preparation of apo-H93G Mb was done by the method of Teale (*33*). An aliquot of imidazole-containing H93G Mb was diluted to a concentration of ∼100 μM in 5 mL of deionized water. The pH of this solution was decreased to 2.3 by the dropwise addition of cold 500 mM HCl. The heme was extracted 3 times by the addition of cold 2-butanone with the organic layer being removed after each extraction. The pH of the apo-protein solution was then increased to 6.0 by the dropwise addition of cold 500 mM NaOH. The apo-H93G Mb was dialyzed overnight in deionized water at 4 °C to remove any remaining 2-butanone. The apo-H93G Mb was reconstituted with hemin by addition of 1 equiv of hemin in 0.1 N NaOH. After standing at 4 °C for 1 h, the sample was concentrated and exchanged into 10 mM potassium phosphate buffer, pH 7.0, on a P6DG gel filtration column. Human H93Y Mb (*9*, *34*) and human H25A heme oxygenase (*17*) were prepared and purified as described previously. Bovine liver catalase was obtained from Sigma. Samples were handled at 4 °C in 100 mM potassium phosphate buffer unless otherwise stated. Heme proteins concentrations were determined by the pyridine hemochromogen method (*35*).

Preparation of the Phenolate Complex of Ferric Octaethylporphyrin. The ferric octaethylporphyrin (OEP) phenolate complex was obtained (*31*) from Fe^{III}(OEP)(Cl) (Aldrich) via cleavage of the μ-oxo dimer with phenol by the method of Tang et al. (*36*).

Spectroscopic Techniques. UV−visible absorption spectra were recorded with a Cary 210 spectrophotometer interfaced to an IBM PC. MCD spectra were measured at 4 °C using a JASCO J500-A spectropolarimeter equipped with a JASCO MCD-1B electromagnet (1.41 T) and interfaced to a Gateway 2000 4DX2−66V PC through a JASCO IF-500−2 interface unit as previously described (*33*). Continuous-wave resonance Raman spectra were obtained at 25 °C with 422.2 nm excitation using an argon-pumped Coherent dye laser with Stilbene 420 dye. Typical laser powers at the sample ranged from 5 to 20 mW, focused to an approximately 100 μ beam waist. A 135° backscattering geometry was used, and the polarization was scrambled prior to entering the monochromator. A SPEX triplemate monochromator was used to disperse collected light onto a Photometrics CCD with a resolution of 2.5 cm^{-1}.

RESULTS

The titration of the exogenous ligand-free ferric H93G Mb with imidazole at neutral pH monitored by resonance Raman spectroscopy is shown in Figure 1. For the ligand-free state, the modes at 1490 cm^{-1} (ν_3) and 1570 cm^{-1} (ν_2) are indicative of a five-coordinate high-spin heme. A minority six-coordinate population is apparent from the band at 1504 cm^{-1} that is evident in the top trace in Figure 1, and more clearly visible in the analogous data of Das and co-workers (*39*). Upon addition of imidazole, the H93G(Im) form shows evidence for six-coordination and a mixture of high- and low-spin. The majority species appears to be six-coordinate high-spin based on the lowering in frequency of ν_3 to 1482 cm^{-1} and ν_2 to 1563 cm^{-1} (Table 1). However, both of these bands

[1] Abbreviations: OEP, octaethylporphyrin; PPIXDME, protoporphyrin IX dimethyl ester; Mb, myoglobin; HO, heme oxygenase; MCD, magnetic circular dichroism.

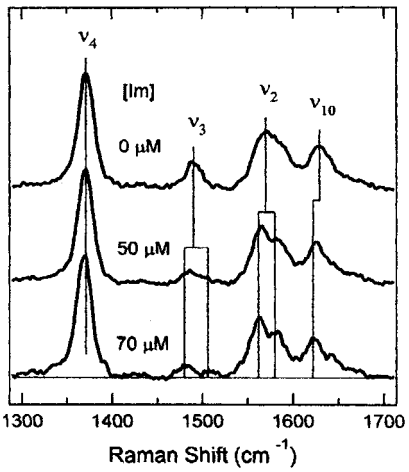

FIGURE 1: Resonance Raman (excitation at 422.2 nm) monitoring of a titration of exogenous ligand-free H93G myoglobin with imidazole. ν_2 and ν_3 are spin state and coordination number marker modes. Samples were 100 μM in 100 mM potassium phosphate buffer, pH 7.0 at 25 °C.

Table 1: Raman Frequencies (cm^{-1}) for Ferric Wild-Type and H93G Myoglobin by Soret Excitation

mode	H93G Mb, pH 7.0	H93G Mb, pH 10.5	H93G(Im) Mb, pH 7.0	wild-type Mb, pH 7.0
$\nu_{C=C}$	1622	1625	1622	ND
ν_{10}	1636	1639	1642	ND
ν_2	1570	1572	1563, 1580	1564
ν_3	1490, 1504	1490	1482, 1507	1483
ν_4	1371	1372	1370	1371
ref	this work	*39*	this work	*9*

show evidence for a low-spin component (the 1507 and 1580 cm^{-1} bands in the lowest trace of Figure 1). In addition, the shoulder that appears at 1640 cm^{-1} when the imidazole adduct is formed may be attributed to a minority six-coordinate form. Both the ν_2 and ν_{10} bands are spectrally congested in spectra of myoglobin with interference from ν_{11}, ν_{19}, and ν_{37} in the 1540−1580 cm^{-1} region and $\nu_{C=C}$ in the 1620 cm^{-1} region. The assignment of water and imidazole as the axial ligands to the six-coordinate heme is supported by the close resemblance of the MCD spectra of the complex to that of native aquo-metMb (*32*). The observation of both high- and low-spin character for H93G Mb upon the addition of imidazole is also seen for native aquo-metMb, offering further support for this coordination assignment (*37*). Bis-imidazole ligation can be ruled out due to the significant difference between the MCD spectrum of the complex (*32*) and that of ferric cytochrome b_5 (*38*). The bis-imidazole complex can be formed by the addition of excess imidazole (60 mM) (*39*).

The UV−visible absorption and MCD spectra of ferric H93G Mb at pH 5.0, 7.0, and 10.0 are seen in Figure 2. The lack of clear isosbestic behavior over the full pH range indicates that more than two species are present over the pH range studied (data not shown). This behavior has been confirmed by resonance Raman data by Das et al. (*39*). At a pH of 7.0, the Soret absorption band is centered at 405 nm. An increase in pH causes it to lose intensity and blue-shift slightly to 403 nm (Figure 2B). As the pH is dropped from 7.0 to 5.0, the Soret feature decreases in intensity and blue-shifts to ~370 nm (Figure 2B). The charge-transfer band at ~600 nm is also a highly variable feature in the spectrum

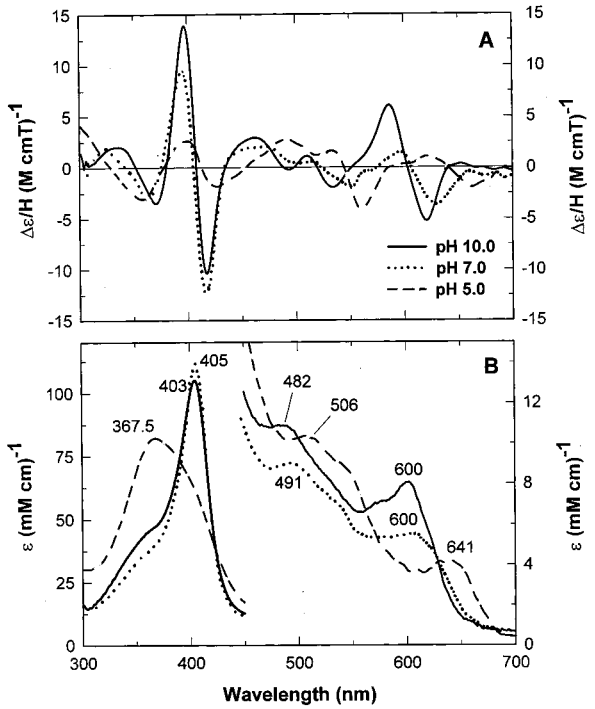

FIGURE 2: Magnetic circular dichroism (A) and UV−visible absorption (B) spectra of exogenous ligand-free H93G myoglobin (35 mM) at pH 5.0 (dashed line), pH 7.0 (dotted line), and pH 10.5 (solid line). All were measured in 100 mM potassium phosphate buffer at 4 °C. The pH was adjusted from 7.0 to 10.5 using 2 N NaOH.

as a function of pH (Figure 2B). As the pH is decreased from 10.0 to 5.0, the wavelength maximum at 600 nm decreases in intensity and shifts to a final position of 641 nm. However, the lack of a clear isosbestic point for this transition precluded determination of a pK_a value.

The H93G Mb heme coordination sphere has been further characterized by MCD spectroscopy at pH 5.0 and 10.0 (Figure 2A). The MCD spectra of the neutral and alkaline pH forms are somewhat similar to one another in line shape and intensity with both varying from that of the acidic form. Comparing the neutral and alkaline species, the most obvious difference between the two forms is the position and intensity of the derivative-shaped bands near 600 nm. The spectral band patterns of these two pH forms remain essentially the same over the remaining section of the wavelength range although, in the visible region (450−700 nm), the neutral pH form is slightly red-shifted relative to the alkaline form. The acidic species exhibits a low-intensity double trough pattern in both the Soret (300−450 nm) and the visible regions. As all three spectra differ distinctly from those of histidine- (*40*) and cysteinate-ligated (*25*) five-coordinate heme complexes, oxygen donor ligation was suspected for the ferric H93G Mb mutant in all three pH states. Precedent for such ligation is found in the exogenous ligand-free ferric derivatives of H175G cytochrome *c* peroxidase (*16*), which has been shown to be predominantly five-coordinate with a single water and five-coordinate with a single hydroxide ligand at pH 5.9 and 7.2, respectively (*23*), and H25A heme oxygenase, which has been proposed to have a single axial ligand of either water or glutamate (*17*).

Figure 3 illustrates the favorable comparison of the acidic form of ferric H93G Mb to the acidic species of horseradish peroxidase (pH 3.1) which has been determined to be five-

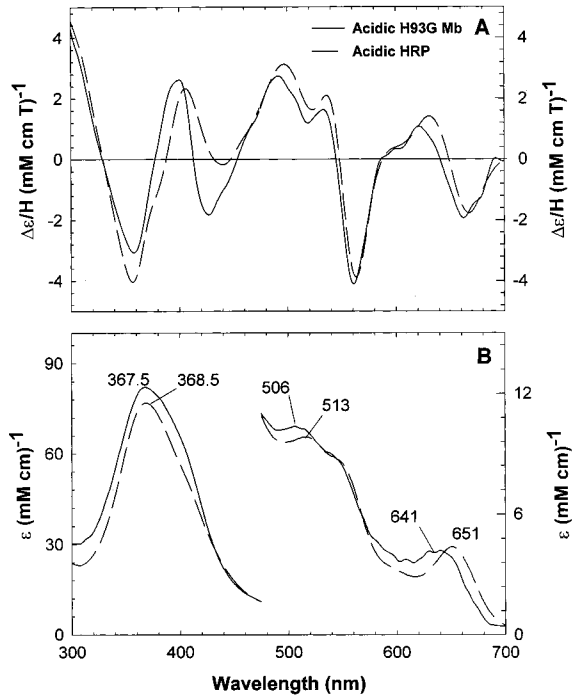

FIGURE 3: Magnetic circular dichroism spectra (A) and UV−visible absorption spectra (B) of exogenous ligand-free ferric H93G myoglobin at pH 5.0 (solid), and acidic ferric horseradish peroxidase at pH 3.1 (dashed). All spectra were measured in 100 mM potassium phosphate buffer at 4 °C.

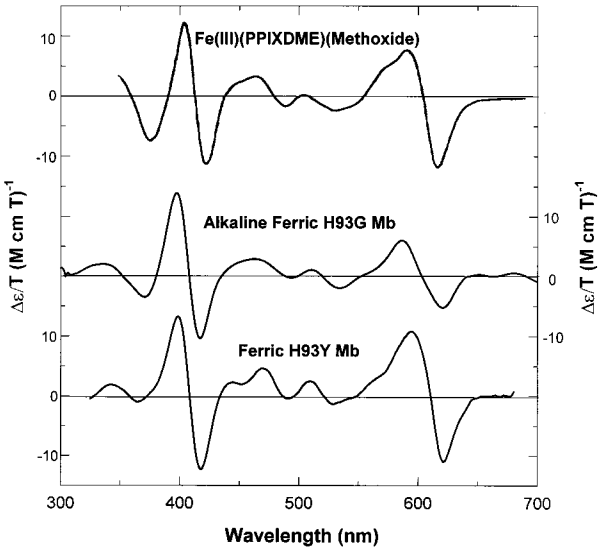

FIGURE 4: Magnetic circular dichroism spectra for Fe^{III}(PPIXDME)-(methoxide) in CH_2Cl_2, replotted from data taken from ref *30*, exogenous ligand-free H93G myoglobin at pH 10.0, and ferric H93Y myoglobin at pH 7.0. The latter two species were measured in 100 mM potassium phosphate buffer at 4 °C.

coordinate high-spin with a single water ligand (*41*) based on spectral comparison with acidic Mb (pH 3.4) (*37*). The alkaline form of exogenous ligand-free ferric H93G Mb exhibits a MCD spectrum that is quite similar to those of two ferric five-coordinate oxygen donor complexes: ferric human H93Y Mb at pH 7.0 (*42*) and the methoxide complex of ferric protoporphyrin IX dimethyl ester (PPIXDME) [Fe^{III}-(PPIXDME)(methoxide)] (*29, 30*) as seen in Figure 4. Previous resonance Raman studies of ferric human H93Y Mb by Adachi et al. determined that the myoglobin mutant was five-coordinate high-spin with a single oxygen ligand

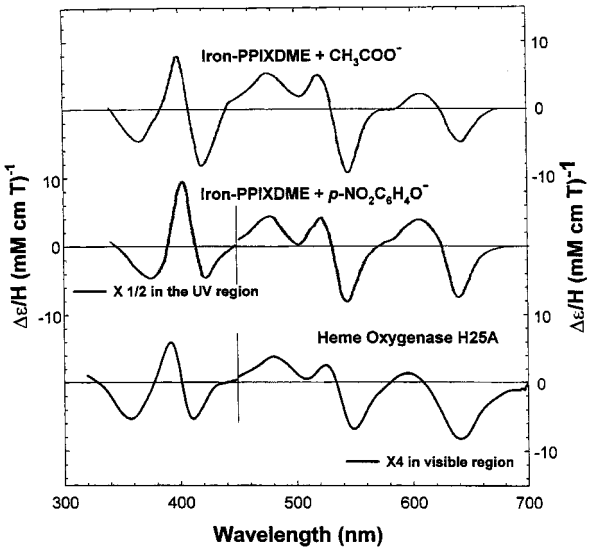

FIGURE 5: Magnetic circular dichroism spectra for Fe^{III}(PPIXDME)-(acetate) and Fe^{III}(PPIXDME)(*p*-nitrophenolate), both in CH_2Cl_2 and replotted using data from ref *30*, and of ferric H25A heme oxygenase which was measured at 4 °C in 100 mM phosphate buffer at pH 7.0. All spectra are plotted on the same scale except for the UV region of the spectrum of Fe^{III}(PPIXDME)(*p*-nitrophenolate) which has been reduced by a factor of 2, and the visible region of the spectrum of the H25A spectrum which has been expanded by a factor of 4.

in the form of tyrosinate (*10*). The alkaline and neutral forms of H93G Mb also compare favorably with the phenolate complex of ferric OEP (*31*) in line shape and intensity, although the spectrum of the latter is blue-shifted due to the less conjugated OEP macrocycle (*43*).

We have also measured the MCD spectrum of ferric human H25A heme oxygenase at neutral pH. Ortiz de Montellano and co-workers have proposed that this cavity mutant contains a five-coordinate heme iron ligated by either water or glutamate based on its distinct spectral differences from known histidine-ligated systems and the lack of a suitable tyrosine in the vicinity of the original histidine ligand (*17*). The MCD spectrum of ferric human H25A heme oxygenase (Figure 5) is somewhat different from those exhibited by alkaline ferric H93G Mb, neutral and alkaline ferric H93Y Mb, Fe^{III}(PPIXDME)(methoxide) (Figure 4), and Fe^{III}(OEP)(phenolate) (*31*). Instead, it is quite similar to the five-coordinate *p*-nitrophenolate and acetate adducts of ferric Fe^{III}PPIXDME (Figure 5) in terms of both band pattern and position of the charge-transfer trough (*29*,*30*).

DISCUSSION

The resonance Raman spectra (Figure 1) of the ferric H93G Mb at neutral pH indicate that the species is primarily a five-coordinate high-spin complex which converts to a six-coordinate complex with both high- and low-spin character upon binding of imidazole. The strong ν_3 mode at 1490 cm^{-1} for the ligand-free complex, typical of a five-coordinate high-spin structure, rules out bis-aquo ligation as the predominant state in the ligand-free species. However, this species could represent the minority population giving rise to the band at 1504 cm^{-1}. The difference between the MCD pattern of the ligand-free neutral complex (Figure 2A) and those of known histidine- and cysteine-ligated heme systems indicates that this species is also not ligated by a nitrogen or sulfur donor

Table 2: Magnetic Circular Dichroism and Absorption Data for Ferric Five-Coordinate Oxygen Donor Complexes of Heme Proteins and Iron Porphyrins

	MCD		absorption		
complex	λ_{max} (nm)	$\Delta\epsilon/H$ (mM cm T)$^{-1}$	λ_{max} (nm)	ϵ (mM cm)$^{-1}$	ref
Fe-PPIXDME + CH_3O^-	398	13.7	401	97.3	*29*, *30*
	530	−2.28	476	14.0	
	618	−12.8	600	9.40	
myoglobin H93Y (pH 5.1−10.5)	398	13.2	402	100	this work
	528	−1.34	480	13.2	
	621	−10.9	598	11.1	
myoglobin H93G (alkaline)	397	13.9	403	104	this work
	534	−1.93	482	10.9	
	621	−5.21	600	8.05	
Fe-OEP + $C_6H_5O^-$	394	4.71	391	86.9	*31*
	536	−5.02	490	10.23	
	626	−6.70	603	6.96	
Fe-PPIXDME + *p*-NO_2-$C_6H_4O^-$	403	20.0	402	115	*32*, *33*
	548	−8.28	500	14.3	
	645	−7.59	621	7.80	
Fe-PPIXDME + CH_3COO^-	402	8.55	400	106	*32*, *33*
	552	−9.69	506	10.5	
	653	−5.04	534	18.7	
			634	15.8	
heme oxygenase H25A	392	5.98	400	96.1	this work
	549	−1.55	492	10.0	
	641	−1.93	620	5.16	

ligand. The pH effect observed in the absorption (Figure 2B) spectra of ferric H93G Mb is best explained by the deprotonation of a water ligand to yield a hydroxide as the fifth ligand as the pH is increased from 5.0 to 10.0. This occurrence would not be unusual for myoglobin as the distal water molecule in wild-type myoglobin also exhibits this behavior (*44*). This deprotonation behavior leads to the proposal that the neutral complex is a combination of a five-coordinate high-spin species with a single hydroxide ligand and a six-coordinate component, possibly a bis-aquo complex. The five-coordinate structure assignment has been substantiated by low-frequency resonance Raman studies at pH 7.4 by Das et al., who observed an isotope-sensitive mode at 575 cm^{-1} (in $H_2{}^{16}O$) which shifts to 551 cm^{-1} in $H_2{}^{18}O$ identifying the ν_{Fe-OH} mode (*39*). The six-coordinate component gives rise to the high frequency ν_3 band at 1504 cm^{-1} seen in Figure 1 (Table 1) with the exact identity of the ligand(s) contributing to this species being currently under investigation.

Comparing the MCD spectrum of the acidic species of H93G Mb to that of the neutral complex (Figure 2A) illustrates the differences between the two complexes. While the spectrum of the neutral species displays derivative-shaped features in both the Soret and visible regions, the acidic species displays double troughs in each region. To further probe the structure of the acidic form, we compared its absorption and MCD spectra with those of acidic horseradish peroxidase (pH 3.1) (Figure 3) and acidic wild-type Mb (pH 3.4) (data not shown). These latter two have been determined by resonance Raman spectroscopy to be five-coordinate high-spin with a single water ligand (*37*, *41*). Both showed a breakage of the iron−histidine proximal bond in the loss of an observable ν_{Fe-His} mode in the deoxy-ferrous state (*37*, *41*), indicating that the fifth ligand observed in the high-frequency resonance Raman was not imidazole. For acidic wild-type Mb, the isotopic sensitivity of the low-frequency resonance Raman bands in D_2O versus H_2O buffer implicated water as the fifth ligand in the acidic complex (*37*). The similarity of the absorption and resonance Raman data for acidic horseradish peroxidase to those of acidic wild-type Mb led to the assignment of the former as a five-coordinate high-spin heme with a single water ligand (*41*). In the case of H93G Mb, the possibility that the protein has unfolded somewhat at pH 5.0 making the absorption and MCD data measured attributable to free heme cannot be completely discounted. However, the similarities in the absorption and MCD data among the acidic derivatives of Mb, horseradish peroxidase, and H93G Mb substantiates our conclusion that the acidic form of ligand-free H93G Mb is a five-coordinate high-spin complex with a single water ligand.

As both the neutral and alkaline species of ligand-free H93G Mb have been determined to be at least partially five-coordinate high-spin with a single hydroxide ligand (with the alkaline species being predominantly five-coordinate high-spin), the differences in their respective absorption and MCD data require clarification. The close similarity of the alkaline species with other characterized five-coordinate oxygen donor complexes (Figure 4) offers further proof that this complex is five-coordinate high-spin with little to no six-coordinate contamination. Resonance Raman results from Das et al. support this view by showing a strong ν_3 mode at 1490 cm^{-1}, typical of a five-coordinate high-spin heme, with little contribution from six-coordinate complexes (*39*). On the other hand, the MCD spectrum of neutral H93G Mb resembles those of the three species in Figure 4 only in band shape, varying in both feature position and intensity, and has a second ν_3 band at 1504 cm^{-1} indicative of six-coordinate character (Figure 1 and Table 1). These variations, coupled with the lack of clean isosbestic points in the pH titration, substantiate the resonance Raman findings that the neutral species while partially five-coordinate high-spin (ν_3 = 1490 cm^{-1}, top trace, Figure 1) contains a minority six-coordinate species (ν_3 = 1504 cm^{-1}, Figure 1 and reference *39*).

Bovine catalase is known to contain a five-coordinate tyrosinate-ligated heme iron (*1*); however, its MCD spectrum is quite distinct from the spectra of the complexes discussed in this study (Figure 4). Fita and Rossman have shown from crystallographic studies that the heme in bovine liver catalase is highly distorted, possibly as a result of contamination in the heme binding site by degraded heme (bile pigment) resulting from the breakage of the heme at the α-meso edge (*1*). Heme distortions have been shown to have drastic effects on the electronic configurations of the iron in other cases as has been recently demonstrated for distorted substituted iron−porphyrin complexes (*45*, *46*). Such distortion of the heme would be expected to significantly affect the spectral properties of catalase as would the presence of degraded heme, explaining the variations between the MCD spectra of catalase and the other five-coordinate oxygen donor ligated hemes discussed in this study. These uncertainties render catalase ineffectual as a comparative tool in the determination of the identity of the fifth ligand of the two mutant heme proteins.

A comparison of the UV−Vis absorption data of all complexes examined in this study can be seen in Table 2. Analysis of these data indicates two groups of complexes with similar peak position, especially the position of the charge-transfer band in the 600−650 nm region. The first group consists of the heme systems ligated by methoxide, phenolate (H93Y Mb), and hydroxide (alkaline H93G Mb) with charge-transfer bands centered around 600 nm. The second group is comprised of the heme complexes with acetate, *p*-nitrophenolate, and a proposed carboxylic acid (H25A HO) with charge-transfer bands centered around ∼620 nm. The distinction between these two groups implies that the UV−Vis absorption data, more specifically, the position of the charge-transfer band, may be sufficient for ligand assignment in the uncharacterized systems. However, similarity of UV−Vis absorption spectra does not always correlate to similarity of coordination complexes. A classic example of this discrepancy can be seen for the ferrous oxy complexes of myoglobin and cytochrome P450cam. While both complexes have similar UV−Vis absorption spectra (*47*, *48*), it is well established that myoglobin has a histidine axial ligand trans to the dioxygen where P450cam has a thiolate. This coordination difference, while not apparent in the UV−Vis absorption data, is obvious from the differences in their respective MCD spectra. As MCD signals can be negative *or* positive, considerably more fine structure can be seen than in absorption spectra. Thus, for empirical comparisons, MCD spectra yield twice the information (i.e., sign and intensity) and therefore afford better "fingerprints" than UV−Vis absorption alone. For this reason, the conclusions drawn within this study are based on the similarity of both the UV−Vis absorption and the MCD spectral data.

The observation that MCD spectral similarities exist between heme systems ligated by hydroxide, methoxide, and phenolate (Figure 4) (with the exception of catalase) is an indication that the electronic properties of these ligands are not sufficiently different so as to alter the electronic structure of the entire ferric heme complex. On the other hand, MCD studies by Hatano and co-workers (*30*) of the ferric *p*-nitrophenolate and acetate adducts of Fe^{III}PPIXDME (Figure 5) indicate that ligands with nonoccupied π^* orbitals have the effect of lowering the energy of the porphyrin to iron charge-transfer transition as a result of interaction of the iron $d\pi$ orbital with the fifth ligand nonoccupied π^* orbital. Hatano and co-workers suggest that this lowered energy is, in turn, translated to a lower energy requirement for the $p\pi$ to $d\pi$ charge-transfer transition and a red-shift of the absorption and MCD features resulting from this transition (*30*). It also appears that this interaction results in an MCD spectrum with less *A*-term character than the spectra of those complexes with ligand lacking vacant π^* orbitals. Comparing the adducts in the Fe^{III}PPIXDME series, the acetate adduct (Figure 5) has the most red-shifted MCD charge-transfer trough at 653 nm with the *p*-nitrophenolate complex next at 646 nm (Figure 5). The methoxide ligand (Figure 4), which lacks nonoccupied π^* orbitals to lower the iron $d\pi$ energy, yields a complex having the most blue-shifted charge-transfer trough at 618 nm (*30*).

A second indicator as to the ligand type is the overall shape of the MCD spectra for the model systems. The MCD spectra of the methoxide adduct display a visible region dominated by a A-term-influenced derivative-shaped feature centered at 600 nm while the MCD spectra of the acetate and *p*-nitrophenolate adducts both exhibit two troughs at ∼550 and ∼645 nm. As other non-oxygen-ligated heme systems such as ferric myoglobin and P450cam have troughs beyond 600 nm in their respective MCD spectra (*47*, *48*), the location of this particular feature in the spectra of the model systems cannot alone be used to make ligand assignments in uncharacterized systems. Instead, comparing both the shape and feature positions of the MCD spectra of the uncharacterized complexes with the spectra of know complexes will result in a more reliable ligand assignment.

For ferric H93Y Mb (Figure 4) and Fe^{III}(OEP)(phenolate) (*31*), we observe that the phenolate ligand tends to induce a spectral signature distinct from that observed for the *p*-nitrophenolate complex (Figure 5) and, instead, similar to that seen for ferric heme complexes with methoxide and hydroxide. This similarity indicates that a strongly electron-withdrawing (through resonance) phenolate *para* substituent is required to make the ligand π^* orbitals available for an energetically favorable interaction with the iron $d\pi$ orbital in order to produce a red-shift of the charge-transfer trough (*30*). This effect has been examined in greater detail in a series of five-coordinated adducts of ferric H93G Mb with thiophenolate and *para*-substituted thiophenolates, including chloro-, methoxy-, methyl-, and nitrothiophenolate, bound to ferric H93G Mb (*32*). Only the charge-transfer band in the spectrum of the *p*-nitrothiophenolate adduct was red-shifted by 10 nm relative to those of the other complexes (*32*). This result supports the proposal that an electron-withdrawing *para*-substituent acting through resonance is required to vacate the π^* orbitals of the ligand which is, in turn, responsible for the shift of the charge-transfer band as proposed by Hatano and co-workers (*30*). With the sensitivity of the position of the charge-transfer band to the character of the axial ligand established both by the above-described study (*32*) and by the work of Hatano and co-workers (*30*), we now use the position of this band and the overall shape of the MCD spectrum to tentatively identify the axial ligand in human H25A heme oxygenase.

The MCD data we have obtained for ferric human H25A heme oxygenase are very similar to those of Fe^{III}(PPIXDME)(*p*-nitrophenolate) (Figure 5) (*29*, *30*). In addition, there

are distinct differences seen in the MCD spectrum of ferric H25A heme oxygenase relative to those of alkaline ferric H93G Mb (Figure 4), ferric H93Y Mb (Figure 4), Fe^{III}-(PPIXDME)(methoxide) (Figure 4), and Fe^{III}(OEP)(phenolate) (*31*). In particular, the presence of two troughs in the visible region of the MCD spectrum of ferric H25A heme oxygenase plus its red-shifted charge-transfer band could indicate that a lowering of the iron $d\pi$ energy has occurred through binding of a ligand with available π^* orbitals. In natural protein systems, the only ligands having such nonoccupied π^* orbitals are the carboxylates of aspartate and glutamate, which, if bound to the heme iron, could induce the red-shift of the charge transfer band and give the varied MCD band shape relative to that of neutral ferric H93G myoglobin, ferric H93Y Mb, Fe^{III}(PPIXDME)-(methoxide), and Fe^{III}(OEP)(phenolate). No less than three glutamyl residues have been previously suggested as candidates for the fifth ligand in ferric H25A heme oxygenase as alternatives to water or hydroxide (*17*). The MCD data presented herein are most consistent with a glutamic acid residue serving as the fifth ligand in ferric H25A heme oxygenase.

CONCLUSIONS

MCD spectroscopy as applied to five-coordinate oxygen donor heme complexes appears able to differentiate between oxygen donor ligands with and without vacant π^* orbitals. As such, the technique may prove to be useful in differentiating between tyrosinate and carboxylate (glutamate and aspartate) ligation in heme proteins. On the other hand, the technique does not distinguish between hydroxide and phenolate (tyrosinate) ligation in such systems. The MCD data of mutant heme proteins and of synthetic model systems presented herein, in combination with data obtained by other physical methods, have led to reasonable heme coordination assignments for the exogenous ligand-free forms of ferric H93G Mb at acidic, neutral, and alkaline pH and the ferric H25A heme oxygenase at neutral pH.

ACKNOWLEDGMENT

We thank Drs. Edmund W. Svastits and John J. Rux for assembling the MCD software.

REFERENCES

1. Fita, I., and Rossman, M. G. (1985) *J. Mol. Biol. 185*, 21−37.
2. Greer, J. (1971) *J. Mol. Biol. 59*, 107−126.
3. Perutz, M. F., Pulsinelli, P. D., and Ranney, H. M. (1972) *Nature (London), New Biol. 237*, 259−263.
4. Pulsinelli, P. D., Perutz, M. F., and Nagel, R. L. (1973) *Proc. Natl. Acad. Sci. U.S.A. 70*, 3870−3874.
5. Nagai, M., and Yoneyama, Y. (1983) *J. Biol. Chem. 258*, 14379−14384.
6. Nagai, M., Yoneyama, Y., and Kitagawa, T. (1989) *Biochemistry 28*, 2418−2422.
7. Egeberg, K. D., Springer, B. A., Martinis, S. A., Sligar, S. G., Morikis, D., and Champion, P. M. (1990) *Biochemistry 29*, 9783−9791.
8. Vardarajan, R., Lambright, D. G., and Boxer, S. G. (1989) *Biochemistry 28*, 3771−3781.
9. Adachi, S., Nagano, S., Ishimori, K., Watanabe, Y., Morishima, I., Egawa, T., Kitagawa, T., and Makino, R. (1993) *Biochemistry 32*, 241−252.
10. Adachi, S., Nagano, S., Watanabe, Y., Ishimori, K., and Morishima, I. (1991) *Biochem. Biophys. Res. Commun. 180*, 138−144.
11. Smulevich, G., Neri, F., Willemsen, O., Choudhury, K., Marzocchi, M. P., and Poulos, T. L. (1995) *Biochemistry 34*, 13485−13490.
12. den Blaauwen, T., Hoitink, C. W., Canters, G. W., Han, J., Loehr, T. M., and Sanders-Loehr, J. (1993) *Biochemistry 32*, 12455−12464.
13. Tu, C. K., Silverman, D. N., Forsman, C., Jonsson, B. H., and Lindskog, S. (1989) *Biochemistry 28*, 7913−7918.
14. Kim, J., Ruzicka, F. J., and Frey, P. A. (1990) *Biochemistry 29*, 10590−10593.
15. Barrick, D. (1994) *Biochemistry 33*, 6546−6554.
16. McRee, D. E., Jensen, G. M., Fitzgerald, M. M., Siegel, H. A., and Goodin, D. B. (1994) *Proc. Natl. Acad. Sci. U.S.A. 91*, 12847−12851.
17. Sun, J., Loehr, T. M., Wilks, A., and Ortiz de Montellano, P. R. (1994) *Biochemistry 33*, 13734−13740.
18. Newmyer, S. L., Sun, J., Loehr, T. M., and Ortiz de Montellano, P. R. (1996) *Biochemistry 35*, 12788−12795.
19. Depillis, G. D., Decatur, S. M., Barrick, D., and Boxer, S. G. (1994) *J. Am. Chem. Soc. 116*, 6981−6982.
20. Decatur, S. M., and Boxer, S. G. (1995) *Biochemistry 34*, 2122−2129.
21. Decatur, S. M., DePillis, G. D., and Boxer, S. G. (1996) *Biochemistry 35*, 3925−3932.
22. Decatur, S. M., Franzen, S., DePillis, G. D., Dyer, R. B., Woodruff, W. H., and Boxer, S. G. (1996) *Biochemistry 35*, 4939−4944.
23. Sun, J., Fitzgerald, M. M., Goodin, D. B., and Loehr, T. M. (1997) *J. Am. Chem. Soc. 119*, 2064−2065.
24. Dawson, J. H., and Dooley, D. M. (1989) in *Iron Porphyrins Part 3* (Lever, A. B. P., and Gray, H. B., Eds.) pp 1−135, VCH, New York.
25. Dawson, J. H., and Sono, M. (1987) *Chem. Rev. 87*, 1255−1275.
26. Roach, M. P., Chen, Y. P., Woodin, S. A., Lincoln, D. E., Lovell, C. R., and Dawson, J. H. (1997) *Biochemistry 36*, 2197−2202.
27. Hawkins, B. K., Wilks, A., Powers, L. S., Ortiz de Montellano, P. R., and Dawson, J. H. (1996)*Biochim. Biophys. Acta 1295*, 165−173.
28. Browett, W. R., and Stillman, M. J. (1979) *Biochim. Biophys. Acta 577*, 291−306.
29. Dawson, J. H., Holm, R. H., Trudell, J. R., Barth, G., Linder, R. E., Bunnenberg, E., Djerassi, C., and Tang, S. C. (1976) *J. Am. Chem. Soc. 98*, 3707−3708.
30. Nozawa, T., Ookubo, S., and Hatano, M. (1980) *J. Inorg. Biochem. 12*, 253−259.
31. Huff, A. M. (1991) Ph.D. Dissertation, *Magnetic Circular Dichroism Investigations of Iron Alkylchlorin Systems*, University of South Carolina.
32. Roach, M. P. (1997) Ph.D. Dissertation *Part I: Spectroscopic Investigations of the Heme Active Site Structure of the Exogenous Ligand-Free Myoglobin Cavity Mutant H93G and Investigations of H93G−Thiolate Adducts as Structural and Mechanistic Model Systems for Cytochrome P450*, University of South Carolina.
33. Teale, F. W. (1959) *Biochim. Biophys. Acta 35*, 543−550.
34. Ikeda-Saito, M., Lutz, R. S., Shelley, D. A., McKelvey, E. J., Mattera, R., and Hori, H. (1991) *J. Biol. Chem. 266*, 23641−23647.
35. Fuhrhop, J.-H., and Smith, K. M. (1975) in *Porphyrins and Metalloporphyrins* (Smith, K. M., Ed.) pp 804−807, Elsevier, Amsterdam.
36. Tang, S. C., Koch, S., Papaefthymiou, G. C., Foner, S., Frankel, R. B., Ibers, J. A., and Holm, R. H. (1976) *J. Am. Chem. Soc. 98*, 2414−2434.
37. Palaniappan, V., and Bocain, D. F. (1994) *Biochemistry 33*, 14264−14274.
38. Vickery, L., Salmon, A., and Sauer, K. (1975) *Biochim. Biophys. Acta 386*, 87−98.

39. Das, T. K., Franzen, S., Pond, A. E., Dawson, J. H., and Rousseau, D. L. (1999) *Inorg. Chem. 38*, 1952−1953.
40. Cheek, J., Coulter, E., Maritano, S., Marchesini, A., and Dawson, J. H. (1996) *Inorg. Chim. Acta 243*, 317−325.
41. Smulevich, G., Paoli, M., DeSanctis, G., Mantini, A. R., Ascoli, F., and Coletta, M. (1997) *Biochemistry 36*, 640−649.
42. Sono, M., Ikeda-Saito, M., and Dawson, J. H., unpublished results indicating that MCD and UV−Visible absorption spectra of ferric human H93Y Mb do not change significantly between pH 7.0 and 10.5.
43. Dawson, J. H., Kadkhodayan, S., Zhuang, C., and Sono, M. (1992) *J. Inorg. Biochem. 45*, 179−192.
44. Iizuka, T., and Morishima, I. (1975) *Biochim. Biophys. Acta 400*, 143−153.
45. Shelnutt, J. A., Song, X. Z., Ma, J. G., Jia, S. L., Jentzen, W., and Medworth, C. J. (1998) *Chem. Soc. Rev. 27*, 31−41.
46. Jentzen, W., Ma, J. G., and Shelnutt, J. A. (1998) *Biophys. J. 74*, 753−763.
47. Alberta, J. A., Andersson, L. A., and Dawson, J. H. (1989) *J. Biol. Chem. 264*, 20467−20473.
48. Dawson, J. H., and Sono, M. (1987) *Chem. Rev. 87*, 1255−1276.

BI9825448